A system approach to selective catalytic reduction deNO$_\text{x}$ monolithic reactor modelling using bond graphs

Jørgen Bremnes Nielsen[a] and Eilif Pedersen[a]

[a]Department of Marine Technology, Norwegian University of Science and Technology, Otto Nielsen vei 10, 7491 TRONDHEIM, Norway

ABSTRACT
Stricter NO$_\text{x}$ emission limits for marine diesel engines have resulted in a market demand for engine external NO$_\text{x}$ reduction solutions. This demand has led to the development of ammonia-based selective catalytic reduction (SCR) deNO$_\text{x}$ systems for marine applications. For SCR systems in general, mathematical modelling and numerical simulation have been essential for increasing knowledge, improving design and developing control algorithms. This has resulted in higher NO$_\text{x}$ reduction performance, reduced NH$_3$ slip and improved transient and start-up performance. Due to the increasing complexity of diesel engine based power systems, it is often argued that system development requires a simulation-based design approach to reduce development cost and increase development speed. For this to be cost-effective, reusable and interchangeable models of appropriate complexity needs to be available. In this paper a system approach is applied to modelling of SCR deNO$_\text{x}$ monolithic reactors. Three models with different levels of fidelity are developed using the bond graph method. The three models are compared by simulating dynamic conditions to uncover differences between the models. In addition, accuracy is investigated by comparing simulation results to measurement data. The contribution in this paper can be summarized to be an exploration of monolith SCR deNO$_\text{x}$ modelling in a system simulation framework, and investigation of the effect of SCR model fidelity on a coupled system performance prediction.

KEYWORDS
SCR deNO$_\text{x}$, System Simulation, Bond graphs

1. Introduction

Stricter regulation of NO$_\text{x}$ emission combined with requirements for reduced fuel consumption is a significant driver for marine diesel engine power system research and development. For the maritime industry, the NO$_\text{x}$ emission limits introduced by IMO MARPOL Annex VI Tier III are now reaching levels where engine internal measures are no longer sufficient and external measures are required. One solution put forward is using ammonia-based selective catalytic reduction (SCR) deNO$_\text{x}$. The use of ammonia-based SCR deNO$_\text{x}$ is a tried and tested method for removal of NO$_\text{x}$ from combustion exhaust gases, initially for stationary sources like boilers, gas turbines and diesel engines for power generation [1, 2]. As regulation of NO$_\text{x}$ from on-road engines has become stricter, automotive applications of SCR systems has become a large topic of research. With the automotive application, challenges such as transient operation, system compactness, and low temperature operation have had to be addressed [3]. SCR systems have also been installed on board ships [4]. Marine applications come with its own challenges such as transient load, low exhaust gas temperature and fuel quality.

CONTACT Jørgen Bremnes Nielsen. Email: jorgen.b.nielsen@ntnu.no

Achieving high SCR system performance in applications where transient operation is the norm has relied and relies heavily on mathematical models and numerical simulation for design support. The importance of mathematical models increases as the regulation become stricter and emission mitigation systems become more complex [5].

The physics and chemistry of an SCR $deNO_x$ system poses a multi-discipline modelling problem including mass and heat transfer, and heterogeneous reaction chemistry. Although these phenomena are of a distributed nature, one-dimensional flow models have proven a successful approach and are widely used for SCR system modelling. One-dimensional flow models of monolith reactors have been used successfully in the automotive industry for predicting monolith catalyst performance. Initially the models were used for investigation of the three way catalyst and later used for SCR system development and performance investigation [6].

The main phenomena occurring in monolith catalyst are mass and energy transfer in the flow direction, diffusion of gas constituents to and from the catalyst wall, diffusion within the catalyst wall, adsorption and desorption of gas constituents, chemical reaction at the surface of the catalyst, heat transfer due to adsorption, desorption, convection, conduction and change of internal energy due to chemical reactions. These phenomena have been included with varying degree in the published models.

Tronconi et al [7] developed an unsteady heterogeneous model of the SCR $deNO_x$ reaction, assuming isothermal conditions. The model included one dimensional mass transfer in the gas phase and a two dimensional mass balance equations in the porous matrix. Tronconi et al [8] further developed the model by removing the isothermal assumption, and by approximating the intraporous concentration profile, simplifying the model. Chatterjee et al [9] introduced a 1D + 1D model, with one dimensional mass transfer in the bulk phase and one dimensional diffusion mass transfer in the catalyst substrate. Arguments are also put forward that intraporous gradients affect the SCR performance in certain operation conditions. Chi and Dacosta [10] published a model where catalyst wall temperature was assumed to vary in the flow direction. In addition the model included the injection and decomposition of urea to ammonia and CO_2. Winkler et al [11] included heat conduction in the gas phase and an approximation for the heat loss due to radiation from the catalyst to the ambient.

A major challenge for SCR system models is simulation speed. Often global kinetic parameters have to be fitted to experimental data, which may be a time consuming process. To achieve required simulation speeds, assumptions of constant velocity and density in the bulk gas phase are generally applied. Emission estimation errors caused by this assumption are generally found to be reduced when tuning the global kinetic parameters to fit measurement data. However, assuming constant velocity and constant density introduces energy conservation errors. This may be especially relevant for marine two stroke application of SCR systems, where due to low exhaust gas temperatures and sulphur containing fuels, the SCR system has to be installed before the turbocharger affecting the coupled system performance.

Current approaches does not focus on, or discuss modelling from a system modelling perspective, where key features are component modeling and total system simulation setup, model reusability, model connectivity and energy conservative modelling. As SCR systems are an integral part of a power system, a system modelling approach may be beneficial. In this paper, a structured examination of SCR system modelling from a systems approach is presented, using the bond graph method. The bond graph method is an energy based, unifying modelling methodology suitable for multi-domain modelling and is used here both for model representation and as a model development framework. Three models with different levels of fidelity are developed. Comparisons of the three models are made with stepped inlet NH_3 concentrations and when connected to a marine two stroke diesel engine model stepping engine load. In addition the accuracy is investigated by comparison with measurement data from an SCR system connected to a marine four stroke engine.

2. Model development

Bulk gas flow is modelled assuming conservation of energy, mass and momentum. In addition handling of gas constituent concentration needs to be included. Modelling SCR deNO$_x$ requires including diffusion from bulk gas phase to catalyst wall, intraporous diffusion, adsorption, desorption, and chemical reactions. The reaction paths for NO$_x$ reduction are complex [12], however two main SCR deNO$_x$ reactions are generally applied, standard reaction and fast. The standard reaction involves NO, while the fast reaction involves NO$_2$ and is considerably faster than the standard reaction. Due to the low engine out NO$_2$ concentration and no marine use of NO oxidation catalysts due to the high sulphur content, the standard deNO$_x$ reaction is dominating. Therefore only the standard deNO$_x$ mechanism is included in the model development. Phenomena to be included in the model are summarized in Figure 1.
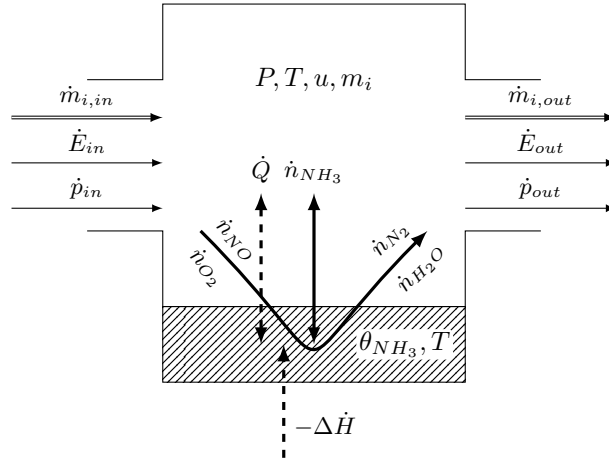

Figure 1. Control volume with compressible fluid flow, surface adsorption, desorption and chemical reactions for the standard deNO$_x$ reaction

The model development is based on assumptions of equal conditions in all catalyst channels, and constant value approximation for flow field properties and concentrations in each control volume.

2.1. One dimensional compressible fluid flow

Several approaches to modelling thermo-fluid flow in bond graphs are available. Thoma [13, 14] introduced a true bond graph using temperature as effort variable and entropy flow as flow variable. Karnopp [15] chose to represent the thermo-fluid flow with pseudo bond graph elements and splitting the flow of energy into two bonds, one hydraulic and one thermal. Brown [16] introduced a bond with two effort variables and one flow variable and corresponding bond graph elements, to represent the flow of energy and mass in a thermo-fluid flow. In this paper the authors have chosen to use the approach of Karnopp.

Strand and Engja [17] expanded the formulation of Karnopp to include momentum resulting in the formulation of one dimensional compressible fluid flow in bond graphs. Strand and Engja did however not consider changing gas compositions. Therefore the approach of Strand and Engja is expanded by including gas constituent concentration information based on the approach of Pedersen [18, 19]. The concentration information is contained in an additional vector pseudo bond where mass flow of a constituent is the flow variable and the mass fraction is the effort variable. The bond graph for a bulk flow control volume is presented in Figure 2 and consists of a hydraulic, a pseudo thermal, a pseudo concentration and a momentum bond representing the conservation of mass, energy, concentration and momentum.
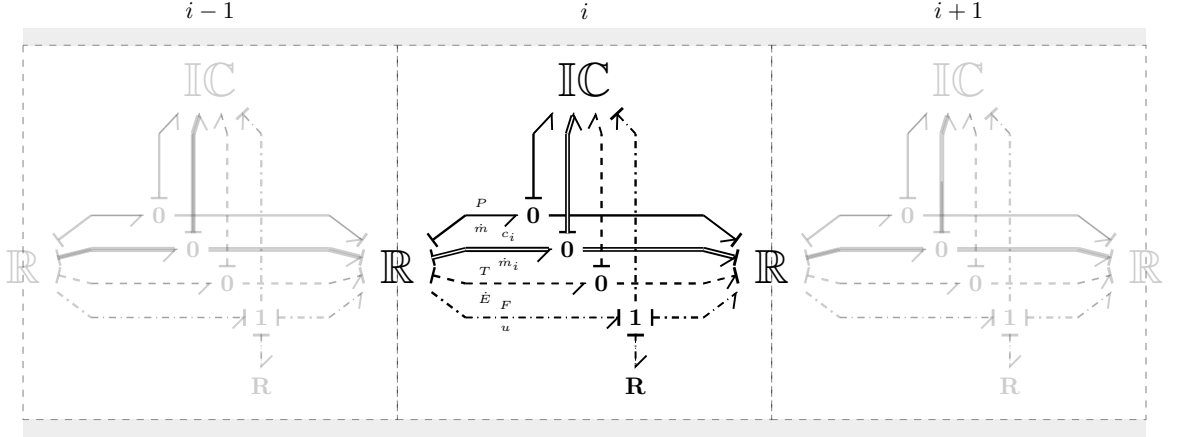
Figure 2. Bond graph for construction of lumped models of general compressible fluid flows with a single control volume highlighted

2.2. Chemical reactions

To the authors knowledge, bond graphs of heterogeneous reactions have not been presented in the literature. Therefore a bond graph of heterogeneous reactions is developed. The development is based on the bond graph representation of homogeneous reactions using true bond graphs with affinity A as effort variable and reaction rate J as flow variable [20]. Figure 3 show a true bond graph representation of the chemical reaction between reactants r_1,r_2 and the products p_1,p_2 with v_r and v_p as stoichiometric coefficient. The true bond graph is connected to the pseudo bonds through a R-field as suggested by Bruun [21].
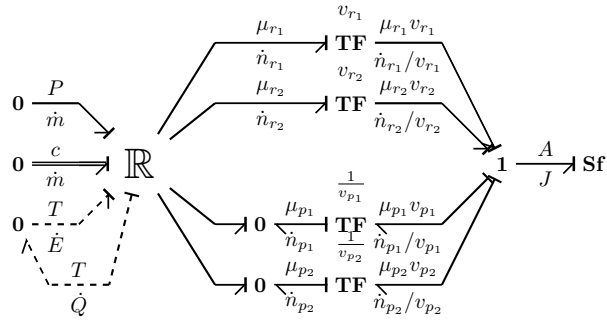

Figure 3. True bond graph for homogeneous chemical reactions connected to pseudo bonds through an R-field

The resulting loss of Gibbs energy is the product $A \cdot J$, where J is the rate of reaction. The affinity A is given by 1

$$A = -\sum_{i=1}^{f+r} v_i \mu_i \tag{1}$$

where the chemical potential μ is given by 2.

$$\mu_i = h_i - T s_i \tag{2}$$

Reaction rates have to be implemented as flow sources (**Sf**) as the reaction rate is not a function of difference in chemical potential between reactants and product, however commonly a function of concentrations and temperature often in the form

of 3.

$$J = kC_1C_2 \tag{3}$$

where

$$k = k^\circ e^{\left(-\frac{E}{RT}\right)} \tag{4}$$

Relationships between the true chemical reaction bonds and the pseudo bonds are handled in the R-field, where flow of energy is given in 5 and 6,

$$\dot{E}_{tot} = \sum_{i=1}^{r+p} h_i \dot{n}_i - T \sum_{i=1}^{r+p} s_i \dot{n}_i \tag{5}$$

$$\dot{E}_{tot} = \dot{E} - \dot{Q} \tag{6}$$

where $\dot{Q}$ is heat released due to entropy production. Mass balance between the pseudo and true bond graph is given by 7.

$$\sum_{i=1}^{r+p} \dot{m}_i = \sum_{i=1}^{r+p} \dot{n}_i M_i \tag{7}$$

Expanding the bond graph to include heterogeneous reaction relevant to SCR deNO$_\text{x}$ requires the addition of adsorption and desorption. Common reaction mechanisms such as the Eley-Rideal and Langmuir-Hinshelwood have to be included. The adsorbed phase and catalyst solid is represented by an additional catalyst control volume C-field. The C-field determines the catalyst temperature and surface coverage based on internal energy and moles of adsorbate. As the catalyst is a solid, pressure is assumed equal to the gas volume pressure removing the need for the pseudo hydraulic bond for the catalyst control volume. The true bond graph for heterogeneous reactions is presented in Figure 4. Note that it is assumed that heat released from adsorption and desorption is added to the catalyst solid and not the gas phase.

Application of the true heterogeneous bond graph requires chemical potential for the gas phase and the adsorbed phase. Determination of the chemical potential for the gas phase is straight forward. Assuming perfect gas, both enthalpy and entropy is available based on tabulated values combined with 8 and 9.

$$h_i = h_0 + c_{p,i}(T_i - T_0) \tag{8}$$

$$s_i = s_0 + c_{p,i} \ln \frac{T_i}{T_0} - R_i \frac{n_i P_i}{P_0} \tag{9}$$

Chemical potential for the adsorbed phase becomes more complicated as it depends on the type of molecule that is adsorbed, on the surface on which it is adsorbed and the interaction between the adsorbate and the adsorbent. There is a body of thermodynamic treatment available where the adsorbent is considered inert [22]. For the adsorbed phase internal energy E_s depends on the independent variables S_s, V_s, A and $n_{s,i}$. Change in internal energy is then

$$dE_s = TdS_s - PdV_s - \phi dA + \sum_i \mu_{s,i} dn_{s,i} \tag{10}$$

Figure 4. True bond graph for heterogeneous chemical reactions with Eley-Rideal and Langmuir-Hinshewood mechanisms. R-field connection to pseudo bond graphs

where A is the surface area of the adsorbate and ϕ is the two dimensional spreading pressure. Chemical potential for the adsorbed phase is given by

$$\mu_s = h_s - Ts_s + \phi\frac{1}{\Gamma} \tag{11}$$

where $\Gamma = n_s/A$. The thermodynamic treatment on the adsorption phase assumes thermodynamic equilibrium between the gas phase and the adsorbed phase [23, 24], $d\mu_g = d\mu_s$. The state of the adsorbate may then be determined based on the state of the gas phase, the adsorption equilibria and the isosteric heat of adsorption. However this approach leads to energy discrepancies for systems not in equilibrium $d\mu_g \neq d\mu_s$. In the presented model, equilibrium is not assumed as temperature of the gas phase and adsorbed phase may differ and the surface coverage is determined by the rate of adsorption, desorption and reaction, and not as a function of pressure and temperature.

The discussion on chemical potential of the adsorbate highlights the challenges related to applying both equilibrium thermodynamics and reaction kinetics to describe a phenomena, as equilibrium thermodynamics and reaction kinetics are generally mutually exclusive. How to address this depends on the purpose of the model and on what model fidelity to apply. In this case the purpose of the model is to predicting the time variation of NH_3 coverage and NO reduction. If the effect on energy flow due to adsorption and desorption is small and the error introduced to energy conservation by not considering it is small, it may be ignored. As the concentration of NH_3 in the exhaust is in the range of 1000 ppm or a mass fraction of approximately 0.1 %, any error in the flow of energy caused by such a small fraction of the total mass and energy flow will result in very small errors in the total energy distribution. It can therefore based on the purpose of the model be concluded that any error in energy flow due to adsorption and desorption will not have any significant effect on performance predictions. With this assumption, a simplified model may be developed.

With no change in chemical potential due to adsorption or desorption, only mass transfer, and associated change in internal energy, between gas phase and catalyst need to be included. Mass transfer is determined by the rates of adsorption, desorption and reaction, now included in the R-field. In addition, heat of reaction is included as a flow source element. The simplified bond graph model is presented in Figure 5.
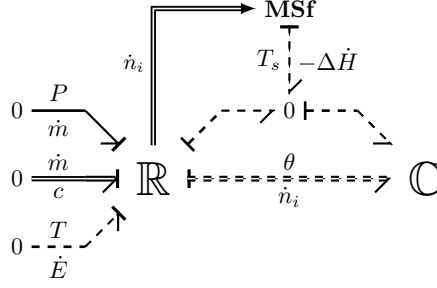
Figure 5. Simplified bond graph for heterogeneous chemical reactions ignoring change in chemical potential for adsorption and desorption and including heat of reaction as a source element

2.3. SCR deNOx modelling

SCR deNO$_x$ performance is affected by intraporous and bulk gas diffusion rates. A diffusion model is required to connect the already presented bulk gas model and the heterogeneous chemical reaction model. Diffusion from bulk gas to catalyst surface has been estimated from the analogy with the Gratz-Nusselts heat transfer problem [25]. The intraporous diffusion has been included by introducing intraporous control volumes. At the catalyst surface boundary between the bulk gas control volumes and the intraporous control volumes, the following quasi steady assumption is made

$$k_{gas}\left(C_b - C_w\right) = D_{ip}\frac{\left(C_w - C_{ip}\right)}{ds/2} \tag{12}$$

where k_{gas} is the convective mass transfer film coefficient, D_{ip} is the intraporous diffusion coefficient, C_b is the bulk gas concentration, C_w is the concentration at the surface boundary, C_{ip} is the concentration in the first intraporous control volume and ds is the intraporous control volume thickness. This relation leads to an algebraic loop which is solved by a low-pass filter.

It is assumed that intraporous mass transfer is purely diffusion controlled. In addition, internal energy for the intraporous control volume is ignored. These assumptions result in an intraporous bond graph with only the concentration bond included. Ignoring internal energy of intraporous control volume results in no energy transfer when mass transfers from the intraporous control volume to the catalyst control volume. The R-fields connecting intraporpous control volumes to catalyst wall control volumes does in this case only contain rate equations for adsorption, desorption and reactions.

The intraporous molar flow is calculated based on concentration gradients according to Ficks first law. The intraporous control volume C-fields calculates the molar volume concentration based on intraporous volumes data available in the literature [8, 26]. Catalyst wall heat capacity is collected to a single thermal control volume, which receives the heat released from chemical reactions and is thermally connected to the bulk gas control volumes via convection. The complete bond graph model is presented in Figure 6. This model will be referred to as the multiple intraporous volume (MIV) model.

2.4. Model reduction by removing intraporous control volumes

Computational speed is always a factor when modelling and simulating. From the system simulation perspective, time frame of interest may be in the minutes to hours range. The goal is therefore to have model capable of running at least in the range of real time to reduce the time for simulation. Therefore a reduced model, with higher simulation speeds is developed in this section. The approach selected here is to replace the intraporous control volumes with an average approximation. This removes a significant number of control volumes, increasing simulation speed.
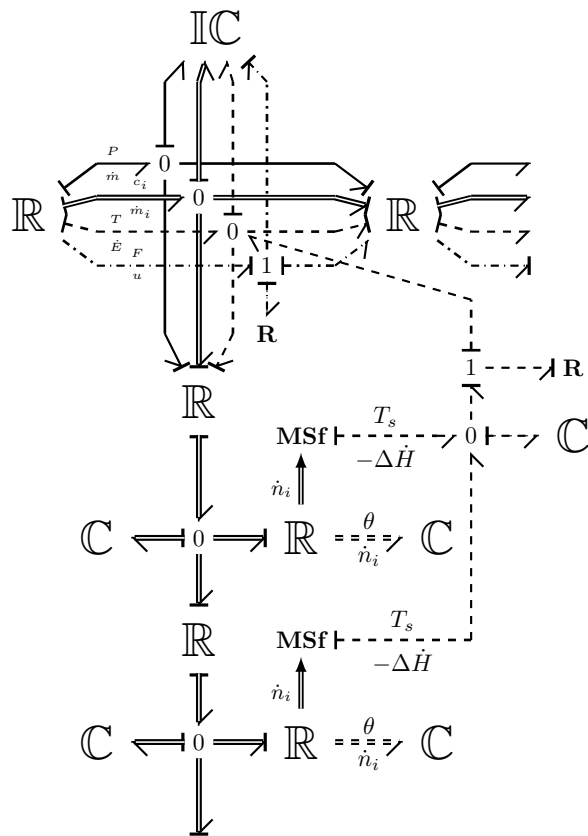
Figure 6. Bond graph representation of unsteady dynamic gas, intraporous diffusion and pore accumulation, and SCR deNO$_x$ heterogeneous chemical reactions

The approximation method is adapted from Tronconi [8] where intraporous concentration and catalyst surface coverage is averaged over the active fraction of the catalyst wall. θ then becomes $\bar{\theta}$ representing the average surface coverage. The resulting bond graph is presented in Figure 7
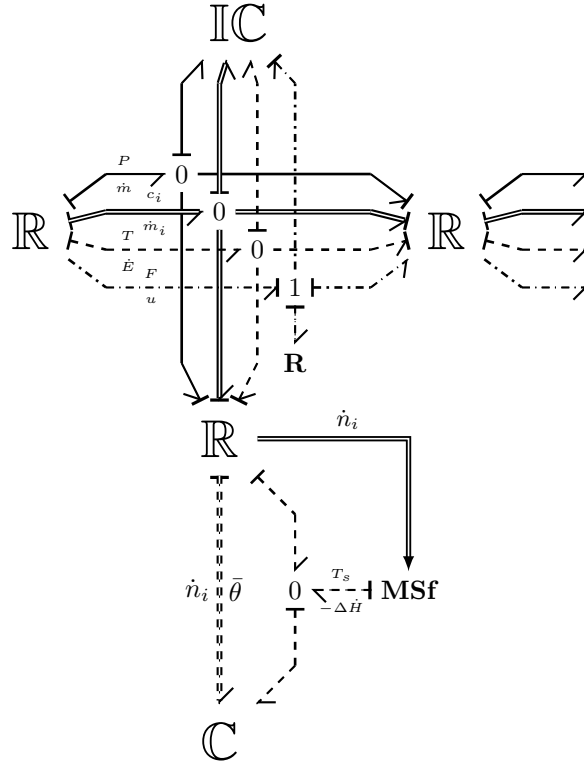

Figure 7. Bond graph representation of unsteady dynamic gas flow, average approximation for intraporous distribution and catalyst surface coverage and SCR deNO$_x$ heterogeneous chemical reactions

With this simplification, the R field is connected directly to the bulk control volume. Mass balance equations for the R-field have to include the bulk to surface mass transfer, and adsorption, desorption and reaction rates. This model will be referred to as the average surface concentration (ASC) model.

2.5. Constant velocity and density model reduction

Further model reduction is possible by disregarding momentum and adopting the constant velocity and constant density assumption throughout the catalyst. This approach violates the conservation of energy, however computational speed gains are significant. Velocity is calculated based on the pressure drop over the catalyst. Density is calculated based on average of upstream and downstream pressure and the inlet composition. Temperature and concentration is set as boundary condition for the first control volume. The average approximation model for the surface coverage and reaction rates is unchanged. The bond graph of constant velocity and density assumption is presented in Figure 8. This model will be referred to as the constant velocity and density (CVD) model.
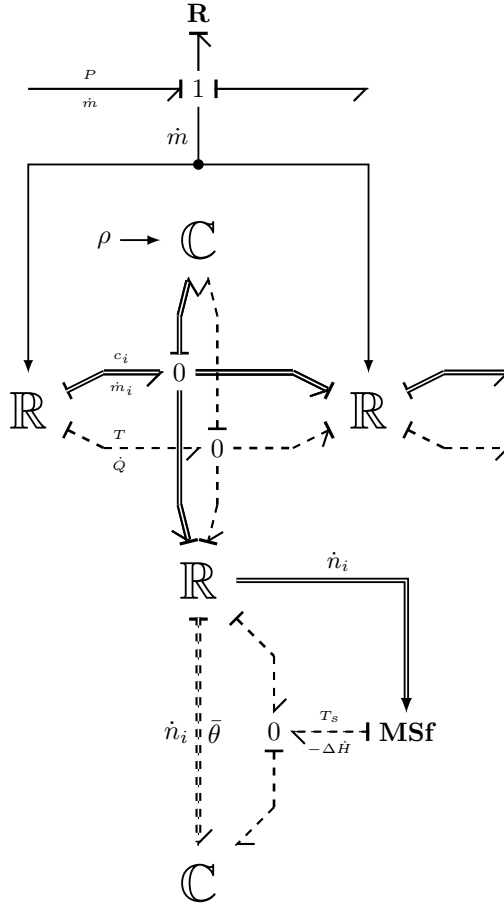
9

Figure 8. Bond graph representation of constant velocity and density gas flow, average approximation for intraporous distribution and catalyst surface coverage and SCR deNO$_x$ heterogeneous chemical reactions

3. Results and discussion

3.1. Model comparison

Before comparing the three models, kinetics of the three models have been fitted to produce the same result when stepping the concentration of NH$_3$. Kinetic parameters available in [7] used with the ASC model are the base case. The MIV and CVD models have then been fitted to the ASC model by global non-linear regression with four different exhaust gas temperatures under typical four stroke exhaust conditions. The NO concentration has been given most weight in the optimization problem as Tronconi [7] presented measurement and simulation data comparison only for NO and not for NH$_3$.

The three models have been compared in a system simulation setting where the SCR system is connected to a two stroke marine diesel engine model [27, 28] in a pre turbine configuration. This comparison is done to determine if there is any difference in total system performance predictions made by the three models. The comparison is made by ramping the engine load from 60 to 70 % in 50 seconds. This is can be considered a fast load change for a marine two stroke engine. The comparison results are presented in Figure 9.

In the results of this load ramp scenario it is observed that neither absolute values or transient performance of engine RPM and turbine speed is affected by the choice of SCR model. It should be noted that the simulation has been preformed without any models for the pipes normally found between the exhaust
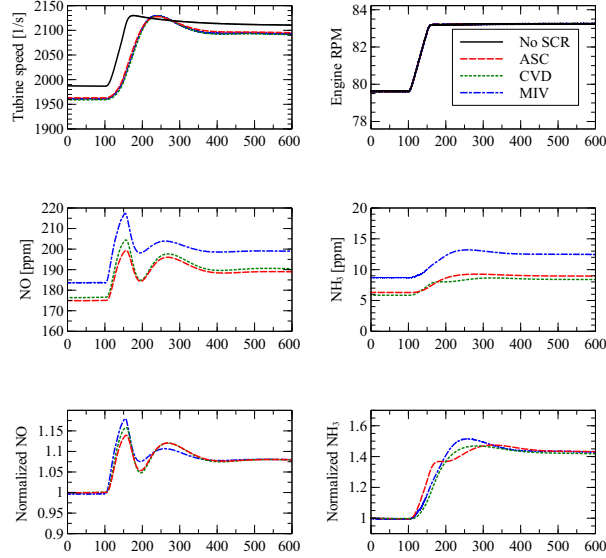
Figure 9. Engine load increased from 60 to 70 % load over 50 seconds. Urea injection is controlled by the SCR control system based on table look up

receiver and the SCR system and the SCR system and the exhaust turbine. This comparison does therefore not cover whether unsteady gas dynamic models are required in these pipes for investigation of turbocharger system stability.

For the emission concentration comparison, minor differences in absolute values of NO and NH_3 are observed between the ASV and CVD. An even larger difference in absolute values are observed between the ASV and MIV models. For easier comparison of dynamics, a normalized comparison is used where the concentration time series are divided by the concentration at time 0 seconds. Differences in concentration dynamics during engine load ramp are observed for all models, with the largest difference found between the MIV and ASV models. Although good fits where achieved, differences in both dynamics and absolute values are observed in the coupled system simulation. Further investigation is required to determine if these differences are caused by the system coupling or if the fitting validity are affected by changing operation conditions and geometry of the catalyst.

3.2. Model validation

The model results have also been compared to test data from an SCR installation on a marine four-stroke three cylinder 500 kW engine running on marine gas oil. Two tests were performed, an urea dosing step test and an engine load step test. The urea step test was performed at four different combinations of engine loads and NH_3 stoichiometric ratios (α). As the SCR system available for the test is an industrial unit without laboratory grade instrumentation there are significant uncertainty associated with the measurement data. The goal of the comparison is therefore to determine if the main dynamics such as shape of the transients and approximate absolute values are captured by the model. Only the average surface coverage model was used in this comparison as it is assumed that the uncertainty in the measurements are larger than the expected differences between the models. Measurement of NO_x was done before and after the SCR unit and NH_3 measurement was performed after the SCR unit. Mass flow was calculated based on inlet air, fuel flow and urea flow measurements. Data from the urea step test was used for curve fitting of parameters via non-linear regression. Results from the curve fitting can be found in Figure 10. The fitting results found in Figure 10 give good NO prediction for all cases except sub-figure a) with 100 % engine load and
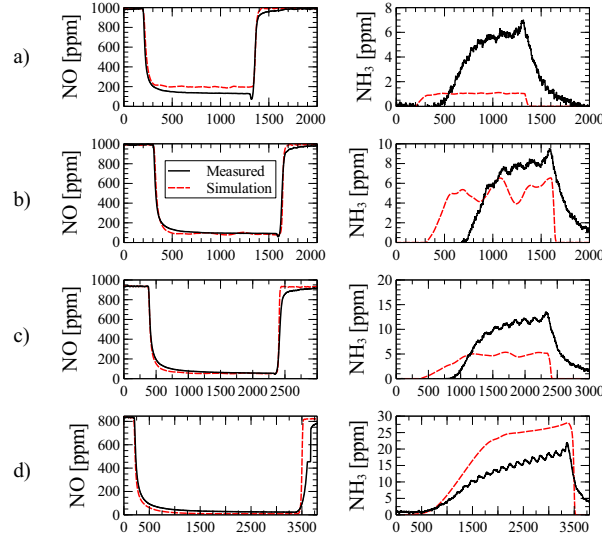
Figure 10. Curve fitting results for model validation. Subfigure a) Engine load 100 %, $\alpha \approx 0.80$. Subfigure b) Engine load 100 %, $\alpha \approx 0.92$. Subfigure c) Engine load 80 %, $\alpha \approx 0.95$. Subfigure d) Engine load 60 %, $\alpha \approx 1.02$.

$\alpha = 0.80$ where the absolute value is off. For the NH_3 concentration prediction there are however significant differences in measured and simulated values. Significant differences include the observed delay between start of injection and time of detection for all cases except sub-figure d) with 60 % engine load and $\alpha = 0.1.02$. It also includes the long tail of the NH_3 when the urea injection is shut down which is not captured by the model. For all cases there are also significant differences in absolute values of NH_3. Based on the observation of the measurement data it can be speculated that there is some sort of NH_3 capture storage and release mechanism that is not covered by the model.

The second test was a engine load step test where the urea dosing control system operated as designed based on a table look up approach. Three load step frequencies were tested, a load step every minute, every second minute and every 15 minutes. The load step was between 50 and 100 % load with constant engine speed. Results of the load step comparison are found in Figure 11.

Again results from Figure 11 show that the model is able to capture the transient shapes and the absolute values of the NO concentration except for some differences in absolute values for the maximum and minimum measured concentrations. However simulation NH_3 results predicts much faster dynamics than what is observed in the measurement data. All dynamics caused by load changes seem to be filtered in the measurement data resulting in no rapid oscillations during fast load changes seen in simulation data of sub-figure b) and c). Probable contributors to the differences observed are the assumptions made about equal conditions in all catalyst channels and no maldistribution of either NO or NH_3. In addition it is assumed that all urea is immediately transformed to NH_3 ignoring the dynamics associated with the transformation of urea to NH_3.

Comparison of the three models has also been performed, checking the assumption that there is no significant difference between the three models. The comparison is made using the kinetic parameters from the model comparison case. The comparison found no major differences in simulation results between the models.
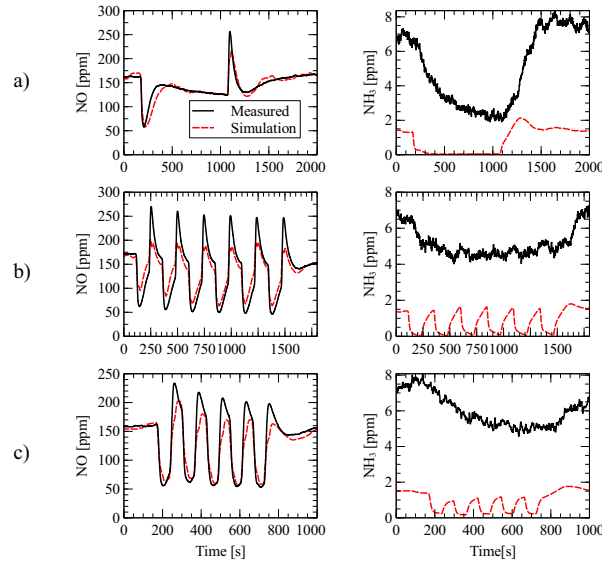
Figure 11. Comparison of measurement data and simulation results for engine load step test. Subfigure a) Load step every 15 minutes. Subfigure b) Load step every 2 minutes. Subfigure c) Load step every minute.

4. Conclusion

Three models with three levels of fidelity have been developed and presented. Using the bond graph method, model development and especially model reduction is structured, and different fidelity models may be used interchangeably. Although interchangeable, the computational cost of each model is significantly different, and using the right model relative to the question of interest is an important modelling decision.

Comparison of the different models showed some differences in NO prediction in a coupled total system simulation, however the three different models gave the same coupled effect on the diesel engine performance. For most cases, using the CVD model will be sufficient for coupled system simulation of marine diesel engines with respect to emision out estimations.

The three models did also perform equally when compared to measurement data. The models captured significant aspects of the performance dynamics when compared to measurement data, however some differences was observed. As the three models performed equally, the cause of differences is believed to be caused by the simplifications introduced by the assumptions on which the models have been developed.

Acknowledgement(s)

References

[1] Nakajima F and Hamada I. The state-of-the-art technology of NOx control. *Catalysis Today* 1996; 29(1): 109–115. .

13

[2] Miller W, Klein J, Mueller R et al. The Development of Urea-SCR Technology for US Heavy Duty Trucks. - 2000; 2000(-): –. .

[3] Koebel M, Elsener M and Kleemann M. Urea-SCR: a promising technique to reduce NOx emissions from automotive diesel engines. *Catalysis Today* 2000; 59(3): 335–345. .

[4] Hug HT, Mayer A and Hartenstein A. Off-Highway Exhaust Gas After-Treatment:Combining Urea-SCR, Oxidation Catalysis and Traps. . URL http://papers.sae.org/930363/.

[5] Weibel M, Schmeißer V and Hofmann F. Model-Based Approaches to Exhaust Aftertreatment System Development. In Nova I and Tronconi E (eds.) *Urea-SCR Technology for deNOx After Treatment of Diesel Exhausts*, chapter 22. New York: Springer Science+Business Media, 2014. pp. 691–707. . URL http://link.springer.com/10.1007/978-1-4899-8071-7{_}22.

[6] Depcik C and Assanis D. One-dimensional automotive catalyst modeling. *Progress in Energy and Combustion Science* 2005; 31(4): 308–369. .

[7] Tronconi E, Lietti L, Forzatti P et al. EXPERIMENTAL AND THEORETICAL IN-VESTIGATION OF THE DYNAMICS OF THE SCR - DeNOx REACTION. *Chemical Engineering Science* 1996; 51(11): 2965–2970.

[8] Tronconi E, Cavanna A and Forzatti P. Unsteady Analysis of NO Reduction over Selective Catalytic Reduction De-NOx Monolith Catalysts. *Industrial & engineering ...* 1998; 5885(x): 2341–2349. URL http://pubs.acs.org/doi/abs/10.1021/ie970729p.

[9] Chatterjee D, Burkhardt T, Bandl-Konrad B et al. Numerical simulation of ammonia SCR-catalytic converters : Model development and application. *SAE transactions* 2005; 114(4): 437–448. .

[10] Chi JN and Dacosta HFM. Modeling and Control of a Urea-SCR Aftertreatment System Reprinted From : Diesel Exhaust Emission Control Modeling. In *SAE Technical Paper Series*. 2005-01-0966.

[11] Winkler C, Flörchinger P, Patil MD et al. Modeling of SCR DeNOx Catalyst - Looking at the Impact of Substrate Attributes Corning Incorporated. *SAE Technical Paper* 2010; (724). .

[12] Busca G, Lietti L, Ramis G et al. Chemical and mechanistic aspects of the selective catalytic reduction of NO x by ammonia over oxide catalysts : A review. *Applied Catalysis B: Environmental* 1998; 18(2): 1–36. .

[13] Thoma JU. Bond graphs for thermal energy transport and entropy flow. *Journal of the Franklin Institute* 1971; 292(2): 109–120. . URL http://linkinghub.elsevier.com/retrieve/pii/0016003271901980.

[14] Thoma JU. Entropy and mass flow for energy conversion. *Journal of the Franklin Institute* 1975; 299(2): 89–96. . URL http://linkinghub.elsevier.com/retrieve/pii/0016003275901313.

[15] Karnopp D. BOND GRAPH MODELING PHILOSOPHY FOR THERMOFLUID SYSTEMS., 1978. URL http://www.scopus.com/inward/record.url?eid=2-s2.0-0017944732{&}partnerID=tZOtx3y1.

[16] Brown FT. Convection bonds and bond graphs. *Journal of the Franklin Institute* 1991; 328(5-6): 871–886. .

[17] Strand K and Engja H. Bond graph interpretation of one-dimensional fluid flow. *Journal of the Franklin Institute* 1991; 328(5-6): 781–793. . URL http://www.sciencedirect.com/science/article/pii/0016003291900547.

[18] Pedersen E. Modelling Thermodynamic Systems with Changing Gas Mixtures. In Granda JJ and Cellier FE (eds.) *1999 International Conference on Bond Graph Modeling and Simulation ICBGM'99*. San Francisco: Society for Computer Simulation International.

[19] Pedersen E. Modelling multicomponent two-phase thermodynamic systems using pseudo-bond graphs. In Granda JJ and Dauphin-Tanguy G (eds.) *2001 International Conference on Bond Graph Modeling and Simulation (ICBGM '01)*. Phoenix: Society for Computer Simulation International.

[20] Auslander DM, Oster GF, Perelson A et al. On Systems With Coupled Chemical Reac-

tion and Diffusion. *Journal of Dynamic Systems, Measurement, and Control* 1972; 94(3): 239. . URL http://dynamicsystems.asmedigitalcollection.asme.org/article.aspx?articleid=1401221.

[21] Bruun K. *Bond Graph Modelling of Fuel Cells for Marine Power Plants*. PhD Thesis, NTNU, Norwegian University of Science and Technology, 2009.

[22] Clark A. *THE THEORY OF ADSORPTION AND CATALYSIS*. New York: Academic Press, 1970.

[23] Hill TL. Statistical Mechanics of Adsorption. IX. Adsorption Thermodynamics and So-lution Thermodynamics. *The Journal of Chemical Physics* 1950; 18(3): 246. . URL http://scitation.aip.org/content/aip/journal/jcp/18/3/10.1063/1.1747615.

[24] Hill TL. Theory of Physical Adsorption. In Frankenburg W, Komarewsky V and Rideal E (eds.) *Advances in Catalysis*, volume 4. Academic Press. ISBN 9780120078042, 1952. pp. 211–258. . URL http://linkinghub.elsevier.com/retrieve/pii/S036005640860615X.

[25] Tronconi E, Forzatti P, Industriale C et al. Adequacy of Lumped Parameter Models for SCR Reactors with Monolith Structure. *AIChE J* 1992; 38(2): 201–210.

[26] Beeckman JW. Measurement of the effective diffusion coefficient of nitrogen monoxide through porous monolith-type ceramic catalysts. *Industrial & Engineering Chemistry Research* 1991; 30(2): 428–430. . URL http://linkinghub.elsevier.com/retrieve/pii/0043164861903428http://pubs.acs.org/doi/abs/10.1021/ie00050a022.

[27] Tasker B, Yum KK, Pedersen E et al. Dynamics of a Marine Propulsion System with a Diesel Engine and a Propeller Subject to Wave. In *Proceedings of the ASME 2015 34th International Conference on Ocean, Offshore and Arctic*. MAY, American Society of Mechanical Engineers,U.S. ISBN 9780791856550. .

[28] Yum KK, Taskar B, Skjong S et al. Simulation of a Hybrid Marine Propulsion System in Waves. In *28th CIMAC World Congress*. Helsinki, Finland.